ELSEVIER

Polymer 40 (1999) 6395–6404

polymer

Dispersion of normal modes in 1,4-*trans*-poly(1,3-pentadiene)

Navnit K. Misra, Deepti Kapoor, Poonam Tandon, V.D. Gupta*

Department of Physics, Lucknow University, Lucknow 226 007, India

Received 15 September 1998; accepted 24 November 1998

Abstract

Calculations of normal modes of isotactic 1,4-*trans*-poly(1,3-pentadiene) and their dispersion within the first Brillouin zone (reduced zone scheme) are reported here. Calculated vibrational frequencies are compared with the reported IR spectroscopic data and a close agreement is found between the two. Characteristic features of dispersion curves, like bunching and repulsion, are observed and discussed. Frequency distribution function derived from dispersion curves is used to calculate the heat capacity in the temperature range 50–450 K. © 1999 Elsevier Science Ltd. All rights reserved.

Keywords: Brillouin zone; Phonon dispersion; Density of states

1. Introduction

The crystal structure of isotactic 1,4-*trans*-poly(1,3-pentadiene)[ITPP], which exists in two distinct conformations, was widely studied by a number of researchers probably because both these chain conformations were experimentally observed to be present in the crystalline state. The first one has the methyl group in *cis* position with respect to the nearest double bond and is called *cis*-model while the other skew-model has the methyl group at the skew position of double bond. Although Bassi et al. [1] showed that the best agreement between observed and calculated intensities of X-ray fiber spectrum is obtained for the *cis*-model, later on Neto et al. [2,3] on the basis of vibrational analysis and Bruckner et al. [4] on the basis of X-ray diffraction analysis concluded that the skew model is preferred over the *cis*-model. Napolitano [5] has made a study of the crystal structure of ITPP using conformational and packing energy considerations and concluded that the polymer chains of ITPP assume a conformation having a skew arrangement of the methyl group i.e. the skew model. Bruckner et al. [6] and Ferro et al. [7] also showed that although the skew conformation is energetically more favorable for a stereoregular sequence, the *cis*-model is more suitable for absorbing configurational defects on the tertiary carbon atom when a rigorous alignment of methyl group is to be preserved. The crystal structure of ITPP was determined by Bassi et al. [1]. It has an orthorhombic unit cell with $a = 19.80 \pm 0.20$ Å, $b = 4.86 \pm 0.05$ Å and $c = 4.85 \pm 0.05$ Å and space group $P2_12_12_1$.

Vibrational analysis of ITPP was reported by Neto et al. [2] using valence force field adopted from polybutadiene. No refinement of force-constants was done. They have also reported the vibrational dynamics of D2 (CD_2) and D8 (fully deuterated) derivatives using same set of force constants [3]. To the best of our knowledge no work on phonon dispersion of ITPP has been reported so far.

In continuation with our earlier work on phonon dispersion and heat capacity of a variety of polymeric systems [8–14], we report here a complete normal mode analysis, including phonon dispersion of ITPP using Urey–Bradley force field which provides a better description of intramolecular interactions because in addition to valence force field the nonbonded interactions are also incorporated. The observed spectral data of Neto et al. [2] were used. The validity of force field and correctness of assignments were checked by frequency shifts in D2 and D8 derivatives. In addition to these, the dispersion curves were plotted and the frequency distribution function obtained from these is used to calculate the heat capacity of ITPP. Dispersion curves have also been reported for the fully deuterated analog.

2. Theory

2.1. Calculation of normal mode frequencies

The calculation of normal mode frequencies was carried

* Corresponding author. Fax: + 91-522-223405.

PII: S0032-3861(98)00855-6

Table 1
Internal coordinates and Urey–Bradley Force constants (mdyn/Å). ν, ϕ, ω, τ denote stretch, angle bend, wag and torsion respectively. Stretching force-constants between the nonbonded atoms in each angular triplet (gem configuration) are given in parentheses

$\nu[C_1–H]$	4.155	$\phi[H–C_1–H]$	0.323(0.36)
$\nu[C_1–C_4]$	3.400	$\phi[H–C_1–C_4]$	0.270(0.20)
$\nu[C_4–H]$	4.340	$\phi[C_1–C_4–H]$	0.485(0.20)
$\nu[C_4–C_M]$	2.500	$\phi[C_1–C_4–C_M]$	0.300(0.20)
$\nu[C_4–C_3]$	2.790	$\phi[C_1–C_4–C_3]$	0.850(0.20)
$\nu[C_M–H]$	4.185	$\phi[H–C_4–C_M]$	0.460(0.20)
$\nu[C_3–H]$	4.774	$\phi[H–C_4–C_3]$	0.510(0.20)
$\nu[C_3=C_2]$	7.500	$\phi[C_M–C_4–C_3]$	0.620(0.20)
$\nu[C_2–H]$	4.706	$\phi[C_4–C_M–H]$	0.420(0.15)
$\nu[C_2–C_1]$	3.800	$\phi[H–C_M–H]$	0.388(0.31)
		$\phi[C_4–C_3–H]$	0.350(0.20)
$\omega[C_3–H]$	0.205	$\phi[C_4–C_3=C_2]$	0.585(0.30)
$\omega[C_2–H]$	0.140	$\phi[H–C_3=C_2]$	0.457(0.175)
$\tau[C_4–C_M]$	0.044	$\phi[C_3=C_2–H]$	0.491(0.30)
$\tau[C_4–C_3]$	0.056	$\phi[C_3=C_2–C_1]$	0.500(0.175)
$\tau[C_3=C_2]$	0.072	$\phi[H–C_2–C_1]$	0.270(0.20)
$\tau[C_2–C_1]$	0.044	$\phi[C_2–C_1–H]$	0.560(0.20)
$\tau[C_1–C_4]$	0.038	$\phi[C_2–C_1–C_4]$	0.520(0.30)

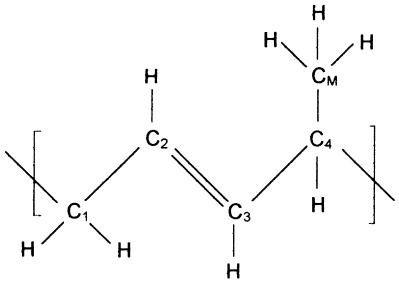

Fig. 1. One chemical repeat unit of ITPP.

out according to Wilson's **GF** matrix method [15–17] as modified by Higgs [18] for an infinite polymeric chain. In brief, the vibrational secular equation, which gives the normal mode frequencies, has the form:

$$|\mathbf{G}(\delta)\mathbf{F}(\delta) - \lambda(\delta)I| = 0 \qquad 0 \leq \delta \leq \pi, \tag{1}$$

where **G** is the inverse kinetic energy matrix, **F** is the potential energy matrix and δ is the vibrational phase

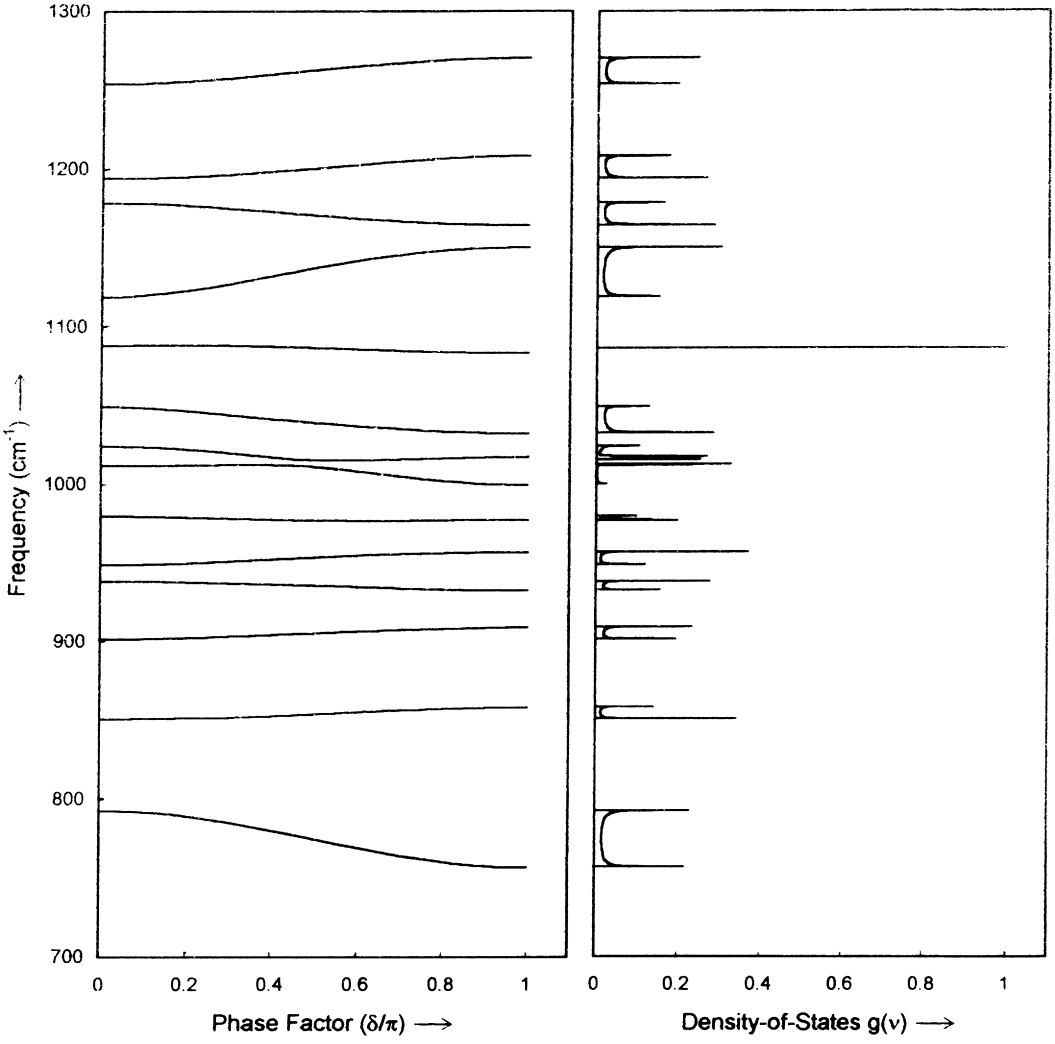

Fig. 2. (a) Dispersion curves of ITPP (1400–700 cm^{-1}); (b) density-of-states g(ν) (1400–700 cm^{-1}).

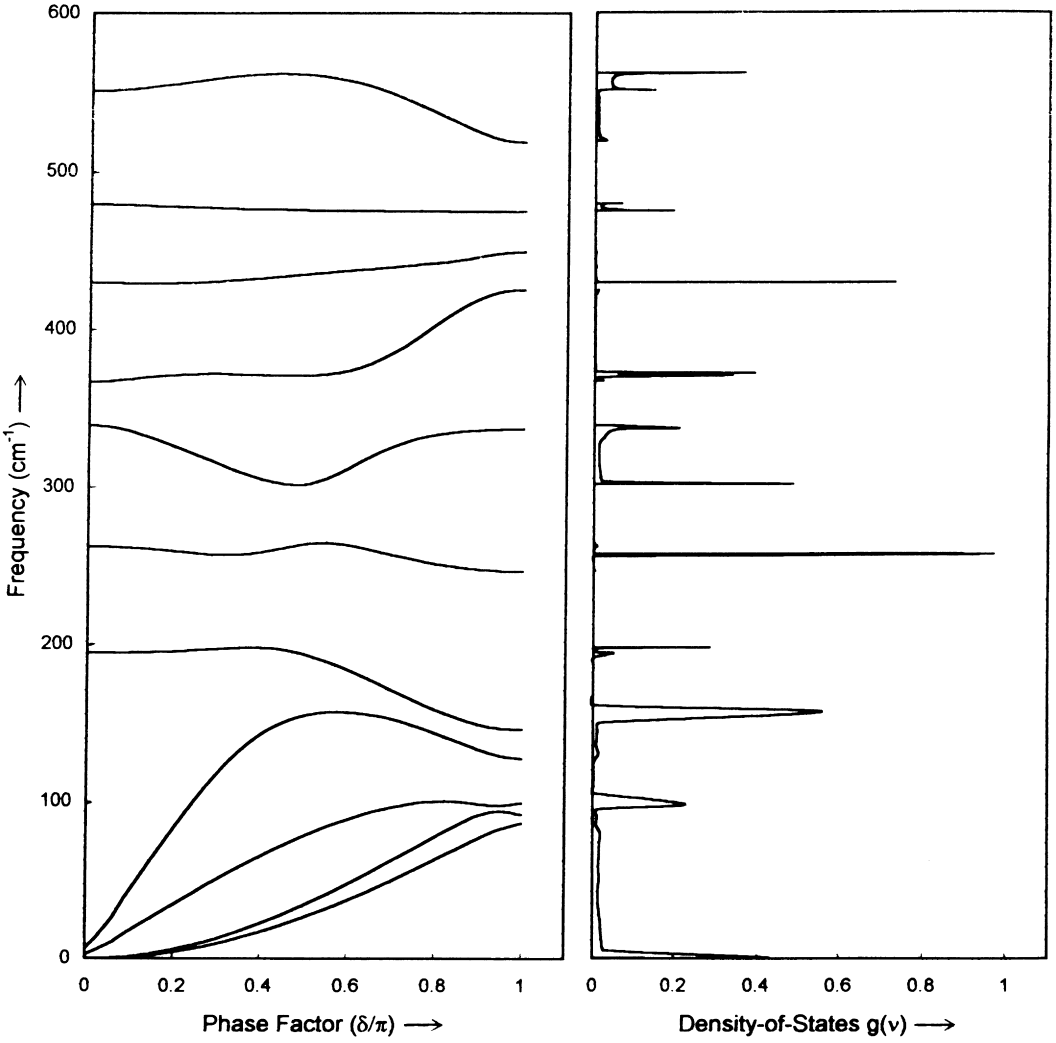

Fig. 3. (a) Dispersion curves of ITPP below 700 cm^{-1}; (b) density-of-states g(ν) below 700 cm^{-1}.

difference between the corresponding modes of adjacent residue units.

The vibrational frequencies $\nu(\delta)$ (in cm^{-1}) are related to the eigenvalues $\lambda(\delta)$ by the following relation:

$$\lambda_i(\delta) = 4\pi^2 c^2 \nu_i^2(\delta). \tag{2}$$

A plot of $\nu_i(\delta)$ versus δ gives the dispersion curve for *i*th mode.

2.2. Calculation of heat capacity

Dispersion curves can be used to calculate the heat capacity of a polymeric system. For a one-dimensional system the density-of-state function or the frequency distribution function is calculated from the relation:

$$g(\nu) = \sum_j (\partial \nu_j / \partial \delta)^{-1}\big|_{\nu_j(\delta)=\nu}. \tag{3}$$

The sum is over all branches *j*. Considering a solid as an assembly of harmonic oscillators, the frequency distribution $g(\nu)$ is equivalent to a partition function.

The constant volume heat capacity C_v can be calculated using Debye's relation:

$$C_v = \sum_j g(\nu_j) k N_A (h\nu_j/kT)^2 \frac{\exp(h\nu_j/kT)}{[\exp(h\nu_j/kT) - 1]^2} \tag{4}$$

with

$$\int g(\nu_j) \mathrm{d}\nu_j = 1. \tag{5}$$

The constant volume heat capacity C_v given by Eq. (4) is converted into constant pressure heat capacity C_p using the Nernst–Lindemann approximation [19]:

$$C_p - C_v = 3RA_0(C_p^2 T / C_v T_m^0), \tag{6}$$

where A_0 is a constant often of universal value [3.9×10^{-9} K mol J^{-1}] and T_m^0 is the estimated equilibrium temperature which is 448 K for ITPP.

Table 2
Methyl group modes

Frequency (cm^{-1})		(Assignment % P.E.D. at $\delta = 0$)	Frequency (cm^{-1})		(Assignment % P.E.D. at $\delta = \pi$)
Calculated	Observed		Calculated	Observed	
2959	2959	$\nu[C_M–H]$ (100)	2959	2959	$\nu[C_M–H]$ (100)
2873	2874	$\nu[C_M–H]$ (100)	2873	2874	$\nu[C_M–H]$ (100)
2873	2874	$\nu[C_M–H]$ (100)	2873	2874	$\nu[C_M–H]$ (100)
1460	1459	$\phi[H–C_M–H]$ (94)	1460	1459	$\phi[H–C_M–H]$ (93)
1460	1459	$\phi[H–C_M–H]$ (95)	1460	1459	$\phi[H–C_M–H]$ (95)
1370	1374	$\phi[H–C_M–H]$ (41) + $\phi[C_4–C_M–H]$ (40) + $\nu[C_4–C_M]$ (11)	1374	1374	$\phi[H–C_M–H]$ (19) + $\phi[C_4–C_M–H]$ (19) + $\nu[C_1–C_4a]$ (12) + $\phi[C_1–C_4–H]$ (11) + $\nu[C_4–C_M]$ (8) + $\phi[H–C_1–H]$ (6) $\phi[C_1–C_4–H]$ (11) + $\nu[C_4–C_M]$ (8) + $\phi[H–C_1–H]$ (6)
940	935	$\phi[C_4–C_M–H]$ (52) + $\nu[C_4–C_M]$ (20)	937	935	$\phi[C_4–C_M–H]$ (51) + $\nu[C_4–C_M]$ (16) + $\tau[(C_2–C_1]$ (7)
860	862	$\phi[C_4–C_M–H]$ (66) + $\nu[C_1–C_4]$ (15) + $\nu[C_4–C_3]$ (11)	868	862	$\phi[C_4–C_M–H]$ (67) + $\nu[C_1–C_4]$ (12) + $\nu[C_4–C_3]$ (10)
820	—	$\phi[C_4–C_M–H]$ (27) + $\nu[C_4–C_M]$ (18) + $\omega[C_3–H]$ (15) + $\nu[C_4–C_3]$ (8) + $\omega[C_2–H]$ (8) + $\phi[H–C_1–C_4]$ (7)	831	—	$\omega[C_3–H]$ (24) + $\phi[C_4–C_M–H]$ (21) + $\phi[H–C_1–C_4]$ (19) + $\tau[C_3=C_2]$ (7) + $\nu[C_4–C_M]$ (5)
730	—	$\nu[C_4–C_M]$ (29) + $\phi[H–C_1–C_4]$ (26) + $\omega[C_2–H]$ (16) + $\phi[C_3=C_2–C_1]$ (6) + $\omega[C_3–H]$ (6)	722	—	$\phi[H–C_1–C_4]$ (36) + $\nu[C_4–C_M]$ (21) + $\omega[C_2–H]$ (18) + $\omega[C_3–H]$ (6)
479	476	$\tau[C_4–C_M]$ (63) + $\tau[C_4–C_3]$ (8) + $\phi[C_1–C_4–C_3]$ (8) + $\phi[H–C_4–C_3]$ (5)	475	476	$\tau[C_4–C_M]$ (44) + $\tau[C_4–C_3]$ (11) + $\phi[H–C_4–C_3]$ (7) + $\tau[C_2–C_1]$ (7) + $\phi[H–C_4–C_M]$ (6)

Table 3
Skeletal modes

Frequency (cm^{-1})		(Assignment % P.E.D. at $\delta = 0$)	Frequency (cm^{-1})		(Assignment % P.E.D. at $\delta = \pi$)
Calculated	Observed		Calculated	Observed	
3026	3025	$\nu[C_2–H]$ (60) + $\nu[C_3–H]$ (40)	3026	3025	$\nu[C_2–H]$ (61) + $\nu[C_3–H]$ (39)
3024	3025	$\nu[C_3–H]$ (59) + $\nu[C_2–H]$ (39)	3024	3025	$\nu[C_3–H]$ (60) + $\nu[C_2–H]$ (39)
2920	2920	$\nu[C_1–H]$ (98)	2920	2920	$\nu[C_1–H]$ (98)
2902	2902	$\nu[C_4–H]$ (98)	2902	2902	$\nu[C_4–H]$ (98)
2842	2841	$\nu[C_1–H]$ (100)	2842	2841	$\nu[C_1–H]$ (100)
1660	1660	$\nu[C_3=C_2]$ (59) + $\nu[C_2–C_1]$ (9) + $\phi[C_3=C_2–H]$ (7) + $\phi[H–C_3=C_2]$ (6) + $\phi[C_4–C_3–H]$ (6)	1664	1660	$\nu[C_3=C_2]$ (59) + $\nu[C_2–C_1]$ (9) + $\phi[C_3=C_2–H]$ (7) + $\phi[H–C_3=C_2]$ (6) + $\phi[C_4–C_3–H]$ (6)
1437	1437	$\phi[H–C_1–H]$ (57) + $\phi[C_2–C_1–H]$ (31) + $\nu[C_2–C_1]$ (6)	1438	1437	$\phi[H–C_1–H]$ (51) + $\phi[C_2–C_1–H]$ (31) + $\nu[C_2–C_1]$ (6)
1345	1344	$\phi[C_1–C_4–H]$ (32) + $\phi[H–C_4–C_3]$ (25) + $\nu[C_1–C_4]$ (19)	1364	1374	$\phi[H–C_M–H]$ (24) + $\phi[C_4–C_M–H]$ (23) + $\nu[C_1–C_4]$ (9) + $\phi[C_1–C_4–H]$ (9) + $\phi[H–C_4–C_3]$ (8) + $\phi[H–C_1–H]$ (6)
1324	1320	$\phi[H–C_4–C_M]$ (22) + $\phi[C_3=C_2–H]$ (17) + $\phi[H–C_4–C_3]$ (11) + $\phi[H–C_2–C_1]$ (8) + $\phi[C_4–C_3–H]$ (7)	1321	1320	$\phi[H–C_4–C_3]$ (33) + $\phi[H–C_4–C_M]$ (25) + $\phi[C_3=C_2–H]$ (8)
1293	1294	$\phi[H–C_4–C_M]$ (21) + $\phi[C_3=C_2–H]$ (15) + $\phi[H–C_4–C_3]$ (11) + $\phi[H–C_2–C_1]$ (10) + $\nu[C_4–C_3]$ (6) + $\nu[C_2–C_1]$ (5) + $\phi[H–C_3=C_2]$ (5)	1276	—	$\phi[C_3=C_2–H]$ (24) + $\phi[H–C_4–C_M]$ (20) + $\phi[C_1–C_4–H]$ (19) + $\phi[H–C_2–C_1]$ (12)

Table 3 (*continued*)

Frequency (cm^{-1})		(Assignment % P.E.D. at $\delta = 0$)	Frequency (cm^{-1})		(Assignment % P.E.D. at $\delta = \pi$)
Calculated	Observed		Calculated	Observed	
1261	1260	ϕ[H–C_3=C_2] (30) + ν[C_3=C_2] (15) + ϕ[C_4–C_3–H] (14) + ϕ[C_2–C_1–H] (13) + ϕ[C_3=C_2–H] (11)	1254	1255	ϕ[H–C_3=C_2] (30) + ϕ[C_4–C_3–H] (15) + ν[C_3=C_2] (14) + ϕ[C_3=C_2–H] (10) + ϕ[C_2–C_1–H] (8) + ϕ[H–C_4–C_3] (5)
1228	—	ϕ[H–C_1–C_4] (24) + ϕ[C_2–C_1–H] (21) + ϕ[C_1–C_4–H] (11) + ν[C_1–C_4] (10) + ϕ[H–C_1–H] (9)	1227	—	ϕ[H–C_1–C_4] (24) + ϕ[C_2–C_1–H] (22) + ϕ[H–C_1–H] (10) + ν[C_1–C_4] (10) + ϕ[H–C_3=C_2] (7) + ϕ[C_4–C_3–H] (5)
1156	1155	ϕ[C_2–C_1–H] (58) + ϕ[H–C_1–C_4] (15) + ϕ[H–C_3=C_2] (6) + ν[C_3=C_2] (6)	1158	1155	ϕ[C_2–C_1–H] (59) + ϕ[H–C_1–C_4] (15) + ϕ[H–C_3=C_2] (5)
1079	1074	ν[C_2–C_1] (21) + ν[C_1–C_4] (16) + ϕ[H–C_2–C_1] (7) + ϕ[C_1–C_4–C_3] (7) + ν[C_4–C_M] (6) + ϕ[C_1–C_4–H] (6)	1049	—	ν[C_1–C_4] (20) + ν[C_2–C_1] (19) + ν[C_4–C_3] (10) + ϕ[C_1–C_4–C_3] (9) + ν[C_4–C_M] (9) + ϕ[C_2–C_1–C_4] (6) + ϕ[C_4–C_M–H] (6)
1022	1022	ν[C_4–C_3] (39) + ϕ[C_4–C_M–H] (21) + ϕ[H–C_4–C_3] (7)	1036	1022	ν[C_2–C_1] (17) + ν[C_1–C_4] (14) + ϕ[C_2–C_1–H] (14) + ϕ[H–C_1–C_4] (11) + ϕ[C_4–C_M–H] (10)
1004	—	ν[C_2–C_1] (34) + ν[C_1–C_4] (16) + ϕ[C_2–C_1–H] (13) + ϕ[H–C_1–C_4] (10) + ϕ[C_4–C_M–H] (10)	998	—	ν[C_4–C_3] (25) + ν[C_2–C_1] (20) + ϕ[C_4–C_M–H] (14) + ν[C_4–C_M] (6) + ϕ[H–C_2–C_1] (6) + ϕ[C_4–C_3=C_2] (5)
965	965	τ[C_2–C_1] (35) + τ[C_3=C_2] (15) + ϕ[C_2–C_1–H] (10) + ω[C_2–H] (9) + ϕ[H–C_1–C_4] (8) + ω[C_3–H] (6)	964	965	τ[C_2–C_1] (33) + τ[C_3=C_2] (12) + ϕ[C_2–C_1–H] (11) + ω[C_2–H] (11) + ϕ[H–C_1–C_4] (10) + ϕ[C_4–C_M–H] (8)
778	777	ω[C_3–H] (42) + ϕ[H–C_1–C_4] (20) + τ[C_3=C_2] (14)	767	777	ω[C_3–H] (39) + ν[C_4–C_M] (17) + ω[C_2–H] (10) + ν[C_4–C_3] (6) + τ[C_3=C_2] (5)
551	548	ϕ[C_4–C_3=C_2] (22) + ϕ[C_2–C_1–C_4] (13) + ϕ[C_M–C_4–C_3] (12) + ϕ[C_1–C_4–C_3] (7) + τ[C_4–C_M] (5) + ϕ[C_4–C_3–H] (5)	518	—	ϕ[C_M–C_4–C_3] (23) + ϕ[C_4–C_3=C_2] (21) + ν[C_2–C_1] (10) + ϕ[C_3=C_2–C_1] (9) + ϕ[C_4–C_3–H] (5)
429	442	ϕ[C_1–C_4–C_3] (16) + ϕ[C_3=C_2–C_1] (13) + ϕ[C_2–C_1–C_4] (12) + τ[C_4=C_M] (11) + ϕ[C_1–C_4–C_M] (8) + ϕ[C_M–C_4–C_3] (6) + ϕ[C_4–C_3=C_2] (5) + ϕ[C_1–C_4–H] (5)	449	442	τ[C_4=C_M] (38) + ϕ[C_1–C_4–C_3] (18) + ν[C_4–C_3] (8) + ϕ[C_1–C_4–H] (6)
367	—	τ[C_4–C_3] (37) + τ[C_2–C_1] (14) + τ[C_4–C_M] (11) + ω[C_3–H] (8) + ω[C_2–H] (7)	425	—	ϕ[C_2–C_1–C_4] (29) + ϕ[C_1–C_4–C_3] (16) + τ[C_4–C_M] (9) + ϕ[C_1–C_4–C_M] (9)
339	330	ϕ[C_M–C_4–C_3] (19) + ϕ[C_3=C_2–C_1] (13) + ϕ[C_1–C_4–C_M] (12) + ϕ[C_2–C_1–C_4] (9) + ϕ[H–C_4–C_M] (6) + ϕ[C_1–C_4–H] (5)	337	330	τ[C_4–C_3] (33) + τ[C_1–C_4] (23) + ϕ[C_3=C_2–C_1] (11) + τ[C_3=C_2] (5)
262	261	τ[C_1–C_4] (26) + ϕ[C_1–C_4–C_M] (19) + τ[C_3=C_2] (15) + τ[C_4–C_3] (10) + ϕ[C_1–C_4–C_3] (8) + ϕ[C_2–C_1–C_4] (7) + ϕ[H–C_4–C_M] (5)	246	261	ϕ[C_1–C_4–C_M] (38) + ϕ[C_M–C_4–C_3] (28) + ϕ[C_3=C_2–C_1] (15)
194	197	ϕ[C_M–C_4–C_3] (35) + ϕ[C_1–C_4–C_M] (23) + ϕ[C_4–C_3=C_2] (14) + τ[C_1–C_4] (11)	145	—	τ[C_3=C_2] (23) + τ[C_2–C_1] (16) + ω[C_3–H] (11) + ϕ[C_2–C_1–C_4] (9) + ϕ[C_M–C_4–C_3] (8) + ϕ[C_1–C_4–C_3] (5)

Table 4
Modes for partially deuterated derivative

Calculated frequency		Observed frequency	(Assignment % P.E.D. at $\delta = 0$)
$\delta = 0$	$\delta = \pi$		
3026	3026	—	$\nu[C_2–H]$ (60) + $\nu[C_3–H]$ (40)
3024	3024	3012	$\nu[C_3–H]$ (59) + $\nu[C_2–H]$ (40)
2962	2962	2960	$\nu[C_M–H]$ (100)
2902	2902	2920	$\nu[C_4–H]$ (99)
2883	2883	2870	$\nu[C_M–H]$ (100)
2882	2882	2870	$\nu[C_M–H]$ (100)
2117	2117	—	$\nu[C_1–D]$ (98)
2110	2110	2090	$\nu[C_1–D]$ (99)
1658	1661	1660	$\nu[C_3=C_2]$ (60)
1459	1459	1455	$\phi[H–C_M–H]$ (95)
1459	1459	1450	$\phi[H–C_M–H]$ (95)
1368	1375	1370	$\phi[H–C_M–H]$ (42) + $\phi[C_4–C_M–H]$ (40) + $\nu[C_4–C_M]$ (11)
1342	1363	1335	$\phi[C_1–C_4–H]$ (35) + $\phi[H–C_4–C_3]$ (27) + $\nu[C_1–C_4]$ (16)
1323	1315	—	$\phi[C_3=C_2–H]$ (21) + $\phi[H–C_4–C_M]$ (18) + $\phi[H–C_4–C_3]$ (10)
1291	1275	1293	$\phi[H–C_4–C_M]$ (27) + $\phi[C_3=C_2–H]$ (13) + $\phi[H–C_4–C_3]$ (11)
1247	1245	1244	$\phi[H–C_3=C_2]$ (39) + $\phi[C_4–C_3–H]$ (20) + $\nu[C_3=C_2]$ (19)
1176	1179	1160	$\nu[C_2–C_1]$ (30) + $\phi[C_2–C_1–D]$ (22)
1126	1112	1126	$\nu[C_1–C_4]$ (40) + $\phi[D–C_1–D]$ (19) + $\phi[C_1–C_4–H]$ (11)
1024	1011	—	$\nu[C_4–C_3]$ (43) + $\phi[C_4–C_M–H]$ (16)
966	951	970	$\phi[D–C_1–D]$ (39) + $\phi[C_4–C_M–H]$ (12) + $\nu[C_2–C_1]$ (12)
942	945	950	$\tau[C_2–C_1]$ (27) + $\phi[C_4–C_M–H]$ (20) + $\omega[C_2–H]$ (17) + $\tau[C_3=C_2]$ (15)
934	933	928	$\phi[C_4–C_M–H]$ (47)
891	909	883	$\phi[C_4–C_M–H]$ (32) + $\phi[C_2–C_1–D]$ (23) + $\nu[C_2–C_1]$ (13) + $\nu[C_4–C_M]$ (11)
859	839	836	$\phi[C_2–C_1–D]$ (50) + $\omega[C_3–H]$ (15) + $\phi[C_4–C_M–H]$ (11)
830	818	836	$\phi[C_4–C_M–H]$ (31) + $\nu[C_4–C_M]$ (15) + $\nu[C_4–C_3]$ (15) + $\omega[C_3–H]$ (12)
773	792	792	$\phi[C_2–C_1–D]$ (23) + $\phi[D–C_1–C_4]$ (20) + $\omega[C_3–H]$ (16) + $\phi[C_4–C_M–H]$ (10)
729	739	—	$\omega[C_3–H]$ (23) + $\nu[C_4–C_M]$ (17) + $\phi[C_2–C_1–D]$ (13)
629	615	—	$\phi[D–C_1–C_4]$ (53)
532	510	515	$\phi[C_4–C_3=C_2]$ (21) + $\phi[C_2–C_1–C_4]$ (16) + $\phi[D–C_1–C_4]$ (15) + $\phi[C_M–C_4–C_3]$ (12)
473	470	452	$\tau[C_4–C_M]$ (68)
401	428	433	$\phi[C_1–C_4–C_3]$ (22) + $\phi[C_3=C_2–C_1]$ (13) + $\phi[C_2–C_1–C_4]$ (11)
360	420	433	$\tau[C_4–C_3]$ (37) + $\tau[C_2–C_1]$ (16)
334	306	300	$\phi[C_M–C_4–C_3]$ (19) + $\phi[C_3=C_2–C_1]$ (15) = $\phi[C_1–C_4–C_M]$ (11)
246	241	—	$\tau[C_1–C_4]$ (28) + $\phi[C_1–C_4–C_M]$ (24) + $\tau[C_3=C_2]$ (15)
193	140	198	$\phi[C_M–C_4–C_3]$ (35) + $\phi[C_1–C_4–C_M]$ (21) + $\phi[C_4–C_3=C_2]$ (14) + $\tau[C_1–C_4]$ (14)

3. Results and discussion

There are 13 atoms in a residue of ITPP giving rise to 39 normal modes of vibration and their dispersion. The vibrational frequencies were calculated for the value of δ ranging from 0 to π in steps of 0.05π. The structural parameters reported by Ferro et al. [7] were used for the calculation of Cartesian co-ordinates. Initially the force constants are transferred from *trans*-polybutadiene [TPBD] [8] and molecules having atoms placed in similar environment and are modified to give "best fit" to the observed IR spectra. Final force constants are given in Table 1. No dispersion is seen in the modes above 1400 cm^{-1} and hence only the modes below this are shown in the Figs. 2(a) and 3(a). The four zero frequencies correspond to acoustic modes representing three translations (one parallel and two perpendicular to chain axis) and one free rotation around the chain axis. The assignment of modes is based on potential energy distribution, relative intensity and profiles of spectral lines and absorption by groups placed in similar environments. The calculated frequencies are compared with the assignments and observed frequencies reported by Neto et al. [2,3]. For the sake of discussion it is convenient to group the vibrational frequencies as methyl group modes and skeletal modes.

Table 5
Modes for the fully deuterated derivative

Calculated frequency		Observed frequency	(Assignment % P.E.D. at $\delta = 0$)
$\delta = 0$	$\delta = \pi$		
2244	2244	2218	$\nu[C_3–D]$ (55) + $\nu[C_2–D]$ (39)
2223	2223	2218	$\nu[C_2–D]$ (58) + $\nu[C_3–D]$ (41)
2139	2139	2145	$\nu[C_M–D]$ (92)
2138	2134	2145	$\nu[C_M–D]$ (98)
2133	2133	2145	$\nu[C_4–D]$ (90)
2119	2119	—	$\nu[C_M–D]$ (96)
2117	2117	—	$\nu[C_1–D]$ (96)
2110	2110	—	$\nu[C_1–D]$ (98)
1616	1621	1620	$\nu[C_3=C_2]$ (66) + $\nu[C_2–C_1]$ (11)
1238	1289	1200	$\nu[C_1–C_4]$ (43) + $\nu[C_2–C_1]$ (14) + $\phi[C_2–C_1–D]$ (11)
1216	1181	1175	$\nu[C_2–C_1]$ (21) + $\nu[C_4–C_M]$ (16)
1156	1134	1139	$\nu[C_4–C_3]$ (31) + $\nu[C_4–C_M]$ (15) + $\phi[D–C_4–C_3$ +] (12)
1083	1070	1100	$\phi[D–C_M–D]$ (23) + $\phi[C_4–C_M–D]$ (23) + $\nu[C_4–C_3]$ (12)
1058	1058	1060	$\phi[D–C_M–D]$ (96)
1056	1056	1055	$\phi[D–C_M–D]$ (97)
1033	1014	1035	$\phi[D–C_1–D]$ (46) + $\phi[C_3=C_2–D]$ (18) + $\phi[C_2–C_1–D]$ (11)
997	972	1006	$\phi[D–C_3=C_2]$ (17) + $\phi[D–C_4–C_M]$ (15) + $\phi[C_4–C_3–D]$ (10) + $\phi[D–C_M–D]$ (10)
938	968	954	$\phi[C_1–C_4–D]$ (23) + $\phi[C_2–C_1–D]$ (16) + $\phi[D–C_4–C_3]$ (10)
855	877	882	$\phi[C_2–C_1–D]$ (34)
847	843	—	$\phi[C_2–C_1–D]$ (35) + $\nu[C_2–C_1]$ (11)
829	799	818	$\phi[D–C_4–C_3]$ (24) + ν $[C_4–C_3]$(16)
794	796	—	$\phi[C_4–C_M–D]$ (26) + $\phi[D–C_4–C_M]$ (15) + $\nu[C_4–C_M]$ (14) + $\phi[D–C_1–C_4]$ (13)
772	785	764	$\phi[C_2–C_1–D]$ (15) + $\phi[C_4–C_M–D]$ (13) + $\phi[C_1–C_4–D]$ (12) + $\phi[D–C_1–C_4]$ (11)
710	710	720	$\tau[C_2–C_1]$ (36) + $\tau[C_3=C_2]$ (16) + $\omega[C_2–D]$ (11)
666	672	—	$\phi[C_4–C_M–D]$ (69)
649	648	647	$\phi[C_4–C_M–D]$ (57) + $\nu[C_4–C_M]$ (13)
625	635	—	$\omega[C_3–D]$ (38) + $\omega[C_2–D]$ (14) + $\nu[C_4–C_M]$ (11)
580	589	—	$\phi[D–C_1–C_4]$ (47) + $\omega[C_3–D]$ (18) + $\tau[C_3=C_2]$ (11)
476	462	473	$\phi[C_4–C_3=C_2]$ (23) + $\phi[C_2–C_1–C_4]$ (16)
391	399	392	$\phi[C_1–C_4–C_3]$ (24) + $\tau[C_4–C_M]$ (11)
364	389	—	$\tau[C_4–C_M]$ (21) + $\tau[C_4–C_3]$ (20) + $\tau[C_2–C_1]$ (14)
321	328	—	$\phi[C_M–C_4–C_3]$ (17) + $\phi[C_1–C_4–C_M]$ (10)
287	276	280	$\tau[C_4–C_M]$ (47) + $\tau[C_4–C_3]$ (13)
225	221	—	$\tau[C_1–C_4]$ (27) + $\phi[C_1–C_4–C_M]$ (22) + $\tau[C_3=C_2]$ (15)
171	132	—	$\phi[C_M–C_4–C_3]$ (36) + $\phi[C_1–C_4–C_M]$ (23) + $\phi[C_4–C_3=C_2]$ (13) + $\tau[C_1–C_4]$ (12)

4. Methyl group modes

ITPP has a methyl group at C_M position (Fig. 1). The modes involving the motion of these atoms are termed as methyl group modes and are given in Table 2. Being highly localized these modes are obtained in the same range as in other polymers. The antisymmetric and symmetric CH stretches are calculated at 2959 and 2873 cm^{-1} which are assigned to peaks at the same value. In *cis*-poly(2-methyl 1,3-pentadiene) [PMPD] [14] these modes are observed at 2964 and 2885 cm^{-1}.

The scissoring vibrations calculated at 1460 cm^{-1} correspond to the observed peak at 1459 cm^{-1} while the symmetric H–C–H deformation with a small contribution from C–C–H bend is obtained at 1370 cm^{-1} (assigned to 1374 cm^{-1}). A major contribution of methyl group rocking is seen in the modes calculated at 940 and 860 cm^{-1} which are assigned to peaks at 935 and 862 cm^{-1} respectively. Although Neto et al. [2] have assigned the observed peaks at 935 and 890 cm^{-1} to the rocking of methyl group, we could get no calculated frequency corresponding to 890 cm^{-1} which is a weak peak in the spectra and our assignment of 862 cm^{-1} mode appears to be correct owing to a close value of this mode in case of PMPD [14]. Both of these modes are dispersive in nature and reach 937 and 868 cm^{-1} at $\delta = \pi$.

The mode calculated at 476 cm^{-1} has a major contribution from C–C torsional vibration. With an increase in δ value the percentage contribution of this mode decreases from 63% to 44% while its contribution in the mode at 429 cm^{-1} (C–C–C bend + C–C torsion at $\delta = 0$) increases

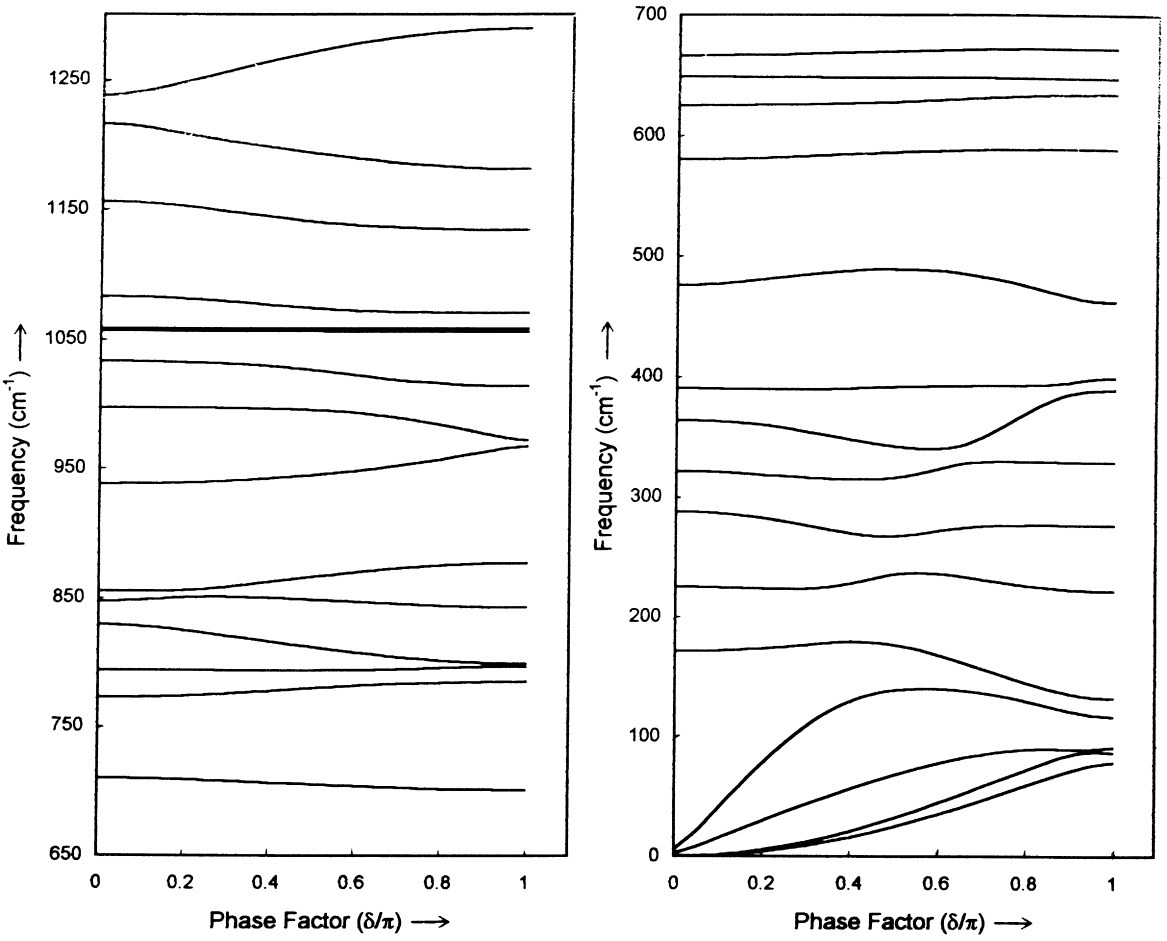

Fig. 4. (a) Dispersion curves of deuterated ITPP (1400–700 cm^{-1}); (b) dispersion curves of deuterated ITPP below 700 cm^{-1}.

from 11% to 38%. In case of PMPD this mode is obtained at 464 cm^{-1}.

5. Skeletal modes

The modes given in Table 3 mainly involve the motion of the atoms of the main chain and are designated as skeletal modes. The CH stretches are mixed in modes calculated at 3026 and 3024 cm^{-1} (assigned to the observed peak at 3025 cm^{-1}). CH_2 stretches are calculated at 2920 and 2842 cm^{-1} and are assigned to peaks at 2920 and 2841 cm^{-1} respectively. These modes appear around the same region in other synthetic polymers as well.

The C=C stretch calculated at 1660 cm^{-1} is used for the structural diagnosis of dienes. It has a higher value for *trans* configuration (1673 cm^{-1} in TPBD [8]) as compared to *cis* configuration (1637 cm^{-1} in *cis* PMPD [14]). The higher value in case of *trans* configuration is because of the lesser steric hindrances between atoms at 1 and 4 position making the double bond stress free. The observed peak at 1437 cm^{-1} is assigned to the scissoring vibration of CH_2 group calculated at the same value. The mode calculated at 1344 cm^{-1} at $\delta = 0$ has a mixed contribution of C–C–H bendings of the backbone and is assigned to the observed peak at 1343 cm^{-1}. At the zone boundary this mode, with a major contribution coming from methyl group bending, reaches 1364 cm^{-1} thereby showing a dispersion of 20 wavenumbers.

The modes calculated at 1261, 1228 and 1186 cm^{-1} have a major contribution of the backbone C–C–H bending vibration. The characteristic mode of dienes involving mainly the C–C torsion vibration with a small contribution from the C–H wag is calculated at 965 cm^{-1} and assigned to a peak observed at the same value.

6. Deuteration

A normal mode calculation for deuterated samples is of great importance in checking the correctness of assignments and validity of the force field. Observed IR spectra for D2(CD_2) and D8(fully deuterated) derivatives of ITPP were reported by Neto et al. [3]. Normal mode calculations for these two species agree with the observed frequency shifts with the same set of force constants. The calculated frequencies along with their assignments are given in Tables 4 and 5 for D2 and D8 derivatives respectively.

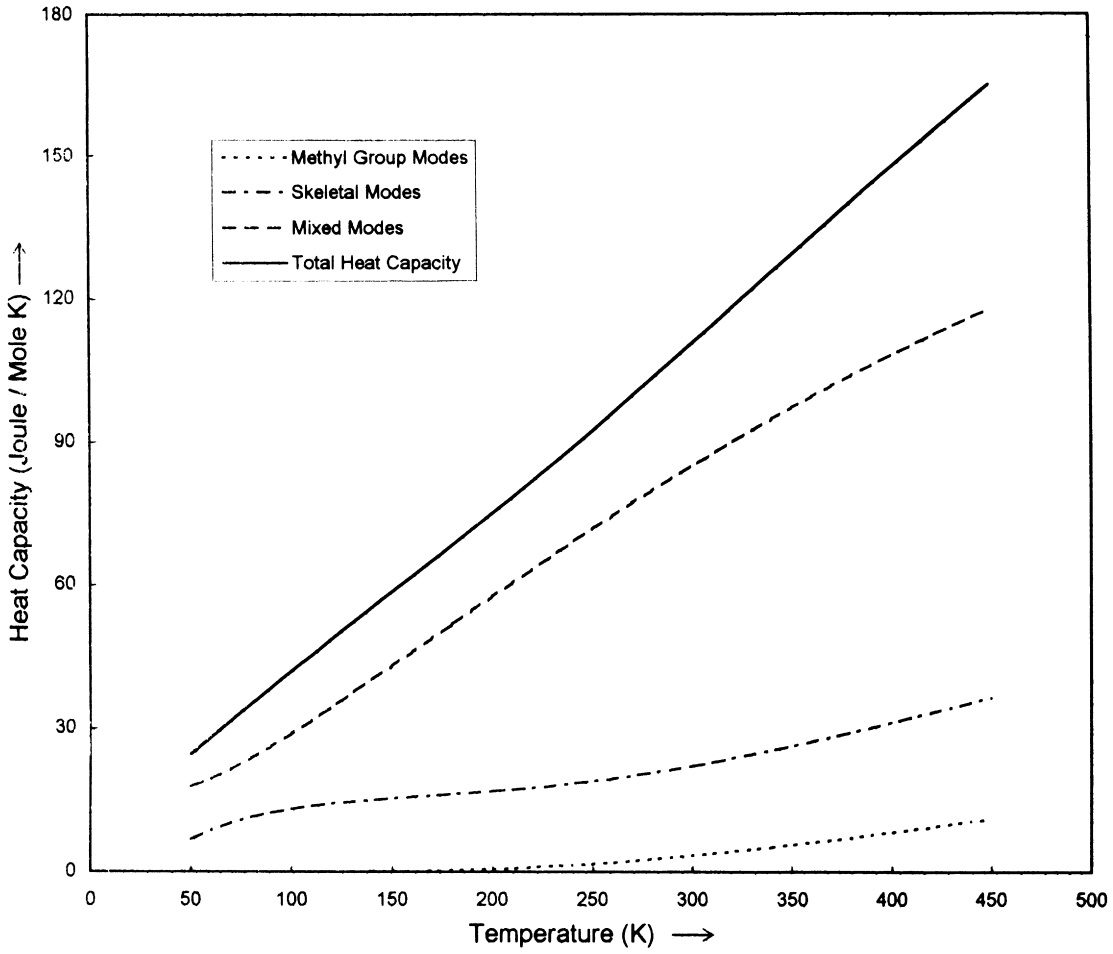

Fig. 5. Variation of heat capacity C_p with temperature.

The C=C stretch calculated at 1660 cm^{-1} for the undeuterated analog gets shifted to 1616 cm^{-1} (corresponding to observed peak at 1620 cm^{-1}) for the fully deuterated sample. For the D2 derivative this mode is almost unaffected and is calculated at 1658 cm^{-1}. In case of partially deuterated (D2) derivative the CD_2 bending has a major contribution in the modes calculated at 1126 and 966 cm^{-1}. A similar mode is obtained at 1100 cm^{-1} for deuterated *trans* polybutadiene. The DCD bendings for D8 derivative are calculated between 1060 and 1035 cm^{-1}. Neto et al. [3] have observed these modes in the same range. The important mode having a mixed contribution from C–C torsion and C–H wags and calculated at 965 cm^{-1} for the undeuterated sample gets shifted to 950 cm^{-1} for D2 and 710 cm^{-1} for the fully deuterated derivative. In case of deuterated TPBD [8] this mode is obtained at 712 cm^{-1}.

7. Dispersion curves

Dispersion curves and frequency distribution function are important for an understanding of thermodynamical and elastic properties of solids. Besides providing the knowledge of density-of-states, dispersion curves give information on the extent of interaction of a mode along the chain in an ordered state. Also a study of these is necessary to appreciate the origin of both symmetry dependent and symmetry independent spectral features. The dispersion curves and the corresponding density-of-states function of ITPP below 1400 cm^{-1} are shown in Figs. 2(a), 3(a) and 2(b), 3(b). It is observed that, as in the case of PMPD, here also the skeletal modes are more dispersive as compared to methyl group modes. Mainly the low frequency modes below 600 cm^{-1} show an appreciable dispersion.

The mode calculated at 551 cm^{-1} at $\delta = 0$ shows a significant dispersion of 33 wavenumbers. Frequency of this mode increases up to 562 cm^{-1} at $\delta = 0.45\pi$ and decreases for higher values of δ to reach 518 cm^{-1} at $\delta = \pi$. Maximum dispersion of 58 cm^{-1} is seen for the skeletal mode calculated at 367 cm^{-1}. This mode has a dominant contribution from backbone torsions and C–H wagging at $\delta = 0$. As δ increases the contribution of both torsion and wag decreases and that of CCC bending starts increasing in this mode. At $\delta = \pi$ this mode reaches 425 cm^{-1} and becomes predominantly CCC bend. In the mode calculated

at 340 cm^{-1} the contribution of CCC bending vibrations increases with an increase in δ value till 0.5π where the frequency becomes 301 cm^{-1} and decreases afterwards. Now with a major contribution coming from C–C torsions it reaches 337 cm^{-1} at $\delta = \pi$.

The dispersion curves for fully deuterated analog are shown in Fig. 4(a),(b). It is clear that the profile of dispersion curves is almost the same and there is an overall downward shift in all the frequencies.

8. Heat capacity

The dispersion curves help us in a better understanding of the thermodynamic properties such as heat capacity of the polymers. The frequency distribution function (density-of-states) which is related to it is derivable from dispersion curves. It expresses the way energy is distributed among various branches of the normal modes. Thus the dispersion curves may be used to correlate the microscopic behavior with the macroscopic properties. In the present case of ITPP the density-of-state curves obtained from dispersion curves are shown in Figs. 2(b) and 3(b). Here we have calculated the heat capacity of ITPP in the temperature range 50–450 K which is shown in Fig. 5. The contributions of pure methyl group modes, pure skeletal modes and a mixture of these i.e. mixed modes has also been calculated separately. It is clear from the figure that maximum contribution comes from the low frequency mixed modes and methyl group modes contribute the least.

Acknowledgements

Financial assistance to N.K.M. and D.K. (under the Junior Research Fellowship scheme), to V.D.G. (under the Emeritus Scientist scheme) from Council of Scientific and Industrial Research and to P.T. from the Department of Science and Technology is gratefully acknowledged.

References

[1] Bassi IW, Allegra G, Scordamaglia R. Macromolecules 1971;4:575.
[2] Neto N, Miranda MM, Benedetti E, Garruto F, Aglietto M. Macromolecules 1980;13:1295.
[3] Neto N, Miranda MM, Benedetti E. Macromolecules 1980;13:1302.
[4] Bruckner S, Di Silvestro G, Porzio W. Macromolecules 1986;19:235.
[5] Napolitano R. Macromolecules 1988;21:622.
[6] Bruckner S, Luzzati S. Eur Polym J 1987;23:217.
[7] Ferro DR, Bruckner S. Macromolecules 1989;22:2359.
[8] Rastogi S, Tandon P, Gupta VD. J Macromol Sci – Phys 1998;37(5):683.
[9] Rastogi S, Gupta VD. J Macromol Sci – Phys 1995;B34(1/2):1.
[10] Bahuguna GP, Rastogi S, Tandon P, Gupta VD. Polymer (UK) 1996;37:745.
[11] Misra NK, Kapoor D, Tandon P, Gupta VD. Polymer J (Japan) 1997;29(11):914.
[12] Misra NK, Kapoor D, Tandon P, Gupta VD. Eur Polym J 1998;34(12)1781.
[13] Gupta A, Tandon P, Gupta VD, Rastogi S. Polymer (U.K.) 1997;38:2389.
[14] Misra NK, Kapoor D, Tandon P, Gupta VD. J Macromol Sci – Phys 1999, in press.
[15] Wilson Jr EB. J Chem Phys 1939;7:1047.
[16] Wilson Jr EB. J Chem Phys 1941;9:76.
[17] Wilson Jr EB, Decius JC, Cross PC. Molecular vibrations: The thoery of infrared and Raman vibrational spectra. New York: Dover Publications, 1980.
[18] Higgs PW. Proc Roy Soc (London) 1953;A220:472.
[19] Roles KA, Wunderlich B. Biopolymers 1991;31:477.